PRAMANA
— journal of
physics

Vol. 41, No. 2,
August 1993
pp. 175–184

L-shell/subshell ionization of Au, Pb and Bi by low energy proton impact

K N PANDEY, D N TRIPATHI, R N CHAKRABORTY and D K RAI
Department of Physics, Banaras Hindu University, Varanasi 221 005, India

MS received 13 October 1992; revised 8 February 1993

Abstract. Proton induced X-ray emission has been used to measure *L*-subshell and total ionization cross-sections of Au, Pb and Bi in the energy range of 200–350 keV. The ionization cross-sections have been extracted using the X-ray spectra and other quantities like fluorescence yields, transition probabilities, relative widths and Coster–Krönig fraction etc. involved in the process. The results have been compared with the cross-sections measured before and discussed in the light of known theories regarding the ion-atom collisions.

Keywords. *L*-shell/subshell ionization; PWBA theory; RPWBA-BC theory; ECPSSR theory

PACS No. 34·50

1. Introduction

Inner shell ionization cross-section for atoms due to charged particle impact are of interest to investigators in radiation damage of biological and other materials, traces in nuclear emulsion, auroral and other atmospheric phenomena as well as to those studying the basic mechanisms of ionization and secondary electron production. Studies regarding the characteristics of the said processes by detecting the emitted X-rays in the bombardment of solid targets with different ions have been carried out extensively in the past few years. Most of these studies are, however, limited to only *K*-shell ionization. Previous work regarding *L*-shell ionization is scarce, as it is more complex comparatively. *L*-shell consists of three sub-shells and the X-rays that are emitted are experimentally not well resolved. The accuracy of the ionization cross-sections are based upon the validity of a set of radiative transition probabilities, fluorescence yields and Coster–Krönig fractions which can be affected by multiple excitation of the target atom. Therefore, a careful analysis of the ion induced X-ray is essential in order to determine the inner shell ionization cross-sections due to ion impact.

In the case of slow moving projectiles which produce inner shell ionization by Coulomb excitation, the theoretical interpretation has undergone a sustained evolution. Corrections for Coulomb deflection, increased binding energy, energy loss and relativistic effects gradually incorporated into these theories have resulted in better agreement with experimental results. Several authors have reported the results of their measurements of X-ray production cross-sections for different elements [1–7] including Au and Pb in the low energy range. The shell/subshell ionization cross-sections have also been measured earlier [8–11].

Measurements in the low energy range, however, show large discrepancies with

the theory especially for the heavier elements [12]. Therefore, accurate measurements are necessary to clarify the behaviour of the inner shell ionization cross-sections in the low velocity limit.

In the present work we measure and analyze the L-subshell and total ionization cross-sections of Au, Pb and Bi due to proton impact in the energy range 200–350 keV. The results have been interpreted in the light of earlier experimental [9, 11, 13] and theoretical [14, 15, 16] studies.

2. Experimental procedure

The beam of proton was extracted from the 400 kV Van de Graff accelerator. The well collimated beam (diameter $\sim 1{\cdot}5$ mm) was allowed to fall on thin target of Au Pb and Bi (density $\sim 200\,\mu g/cm^2$) and mounted at 45° to the beam direction at the centre of the evacuated ($\sim 10^{-6}$ torr) scattering chamber [17]. The Au target was self-supporting; while the Pb and Bi targets were deposited on mylar backing ($\sim 700\,\mu g/cm^2$ thick). The L X-rays, emitted as a result of the inelastic collision, passed through a 6 μm hostaphane foil window and 2 cm air gap. The L X-rays were detected by a Si(Li) detector (having a energy resolution of ~ 200 eV FWHM at 5·9 keV) placed at 90° to the beam axis. Proton beam current (maximum) up to 160 nA were employed for bombarding the targets. The spectrum of the emitted X-rays for each element at 300 keV proton energy is shown in figures 1–3.

3. Determination of L-shell and subshell ionization cross-sections

The L X-ray energy spectrum may be divided into three main groups: the L_α, L_β and L_γ. The L_α has weaker L_l and L_η lines in its tail. The L_β lines are resolved into their

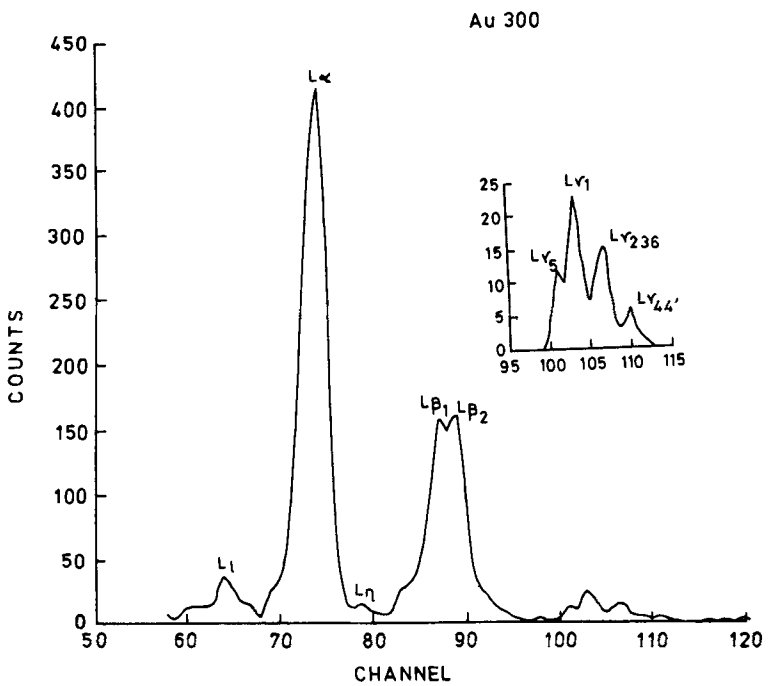

Figure 1. Proton impact L-shell X-ray sepctrum of Au at 300 keV.

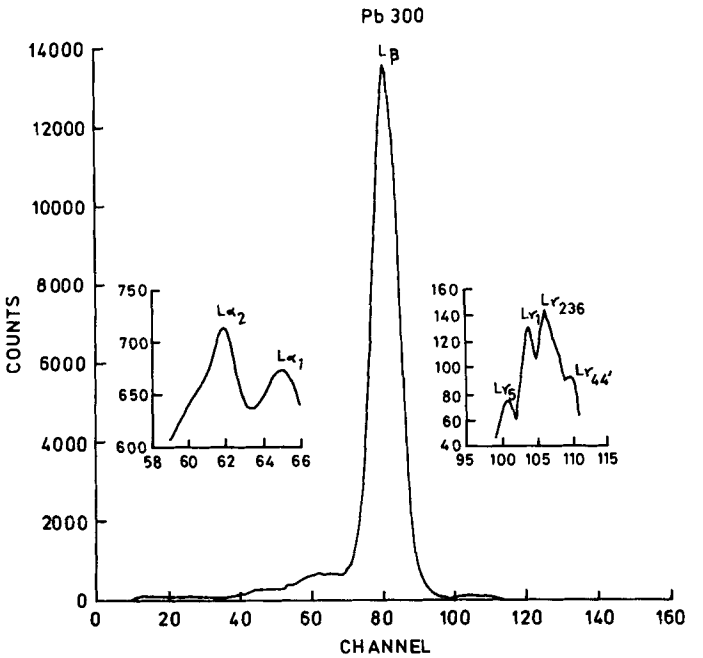

Figure 2. Proton impact *L*-shell X-ray spectrum of Pb at 300 keV.

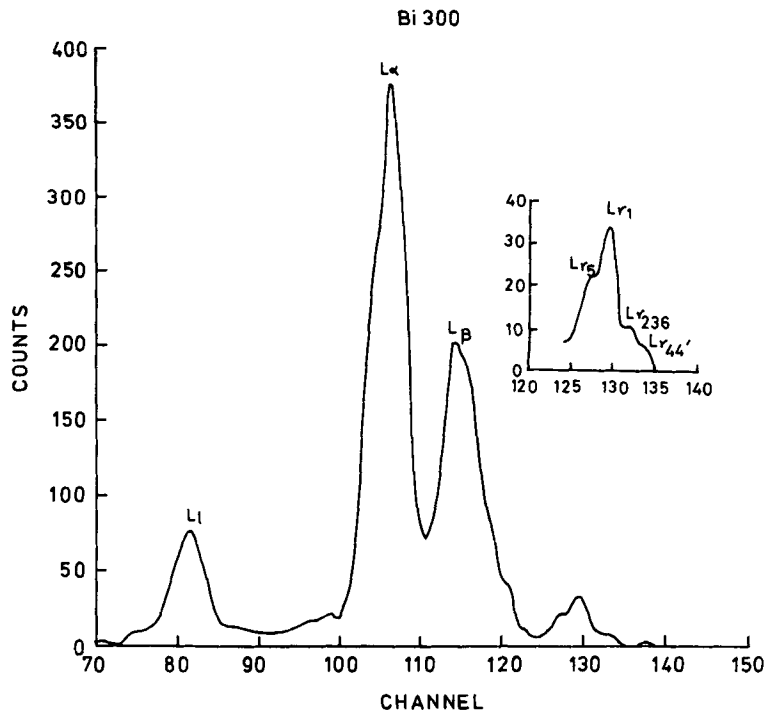

Figure 3. Proton impact *L*-shell X-ray spectrum of Bi at 300 keV.

components for lower impact energies only, while L_γ lines could not be resolved into their components. L X-ray emission has been taken to be isotropic [10].

Experimental L_j X-ray production cross-sections $\sigma^x_{L_j}$ were determined from the expression given below [18]

$$\sigma^x_{L_j} = Y_{L_j} A_2 4\pi / N_p N_0 (\rho t) \Omega 2^{1/2} \varepsilon_{L_j} C_{L_j}, \tag{1}$$

where Y_{L_j} is the L_j X-ray yield, A_2 is the target mass, N_p is the number of charged particles to which the target has been exposed, N_0 is the Avogadro's number, ρt is the areal density of the target, Ω is the solid angle of the Si(Li) detector, ε_{L_j} is the Si(Li) detector efficiency and C_{L_j} denotes the absorption correction for L_j X-rays in hostphane-foil chamber window and air. The mass absorption coefficient required for evaluating C_{L_j} has been obtained using the table of Storm and Israel [19].

The L_α, L_β, L_γ, L_l and L_η lines are clearly separated in the observed spectrum. (see figures 1–3). The measured L_α, $L_{\gamma 1}$, $L_{\gamma 236}$ and $L_{\gamma 44'}$ X-ray production cross-sections are related with L_i subshell ionization cross-sections $\sigma^{exp}_{L_i}$ $(i = 1, 2, 3)$ by the following relation [18];

$$\sigma^{exp}_{L_1} = S_1 \sigma^x_{L\gamma 2344'} / S_{1\gamma 2344'} \omega_1, \tag{2}$$

$$\sigma^{exp}_{L_2} = S_2 \sigma^x_{L\gamma 1} / S_{2\gamma 1} \omega_2 - f_{12} \sigma^{exp}_{L_1} \tag{3}$$

$$\sigma^{exp}_{L_3} = S_3 / S_{3\alpha\omega_3} [\sigma^x_{L_\alpha} - \omega_2 (f_{12} \sigma^{exp}_{L_1} + \sigma^{exp}_{L_2}) S_{2\eta} / S_2] - \sigma^{exp}_{L_1} (f_{12} f_{23} + f_{13} + f'_{13}) - \sigma^{exp}_{L_2} f_{23} \tag{4}$$

where $\omega_i (i = 1, 2, 3)$ are the L_i subshell fluorescence yields, $f_{ij} (i, j = 1, 2, 3$ with $i < j)$ are the non-radiative Coster–Krönig yields, f_{13} is the radiative Coster–Krönig yield, $S_i (i = 1, 2, 3)$ are the total L_i radiative rates and S_{ij} are the radiative rates of L_{ij} transitions. The value of ω_i and f_{ij} were extracted from the table of Krause [20] and S_{ij} from the table of Scofield [21]. The required $L_{\gamma 2344'}$ yield was obtained from the expression as given below:

$$Y_{L_{\gamma 2344'}} = Y_{L_{\gamma 23644'}} - Y_{L_{\gamma 1}} S_{2_{\gamma 6}} / S_{2_{\gamma 1}}. \tag{5}$$

A detailed description regarding the determination of quantum efficiency of the solid state detectors has been given by Buras and Gerward [22]. It is quite obvious from figure 15 (page 108) of that reference that in the X-ray energy range of interest in the present work viz; 3 to 15 keV, the efficiency is almost unity.

The major sources of experimental uncertainties included for determining the total experimental error in the total ionization cross-sections are the following,

(i) projectile energy (2·5%), (ii) target areal density (2·2%), (iii) absorption corrections (5–10%), (iv) solid angle (1·4%), and (v) counting statistics ($\leqslant 10\%$)

On combining these uncertainties quadratically, the final uncertainties in $\sigma^x_{L_i}$ were found to be 6–10, 6–11 and 6–14% for L_α, $L_{\gamma 1}$ and $L_{\gamma 2344'}$ respectively. The atomic parameters (ω_i, S_{ij} and f_{ij}) introduce systematic uncertainties into $\sigma^{exp}_{L_i}$ as has been pointed out by several authors (for example, [23, 24]). However, these are difficult to quantify and consequently, following normal practice, were excluded from the error calculations. The final uncertainties in $\sigma^{exp}_{L_i}$ for protons incident on Au are 6–14% for L_1, 13–14% for L_2 and 8–17% for L_3.

4. Results and discussion

Gold: The measured subshell (σ_{L_1}, σ_{L_2} and σ_{L_3}) and total (σ_L) ionization cross-sections due to proton impact in the energy range of 200–350 KeV are given in table 1 and shown in figure 4. The cross-sections measured by Datz *et al* [9], Kiss *et al* [11] and the available theoretical results due to Pandey *et al* [14] (PWBA), Cohen and Harrigan [15] (ECPSSR) and Chen and Crasemann [16] (RPWBA-BC) are also given for the sake of comparison. Our results of σ_{L_1} and σ_{L_2} at 250 keV are almost half of that due to Datz *et al* [9] but are in good agreement with the calculated values reported by Chen and Crasemann [16] (RPWBA-BC) as well as Cohen and Harrigan [15] (ECPSSR). Present results of σ_{L_3} are however, in close agreement with both earlier observed and theoretically calculated cross-sections. At 350 keV incident energy, our measured values for σ_{L_2} and σ_{L_3} are in good agreement with the results of Datz *et al* [9]. Present measurements regarding σ_{L_1} σ_{L_2} and σ_{L_3} at 200 keV energy are in quite good agreement with the previous results. The results of our total *L*-shell ionization cross-sections (σ_L) are in very good agreement ($\mp$ 15%) with the earlier results of experiment [9, 11] and theory (ECPSSR and RPWBA-BC) at 200 keV.

The subshell ionization cross-section ratios viz: $\sigma_{L_1}/\sigma_{L_2}$, $\sigma_{L_2}/\sigma_{L_3}$ and $\sigma_{L_1}/\sigma_{L_3}$ are listed in table 4. Our measured values of $\sigma_{L_1}/\sigma_{L_2}$ are in agreement with the calculated ratios in the entire energy range and with the earlier measurements in the 250–300 keV range. But for 200 keV and 300 keV incident energy our results deviate from the earlier measurements. For $\sigma_{L_2}/\sigma_{L_3}$ the present values are in good agreement with the previously reported results.

Lead: Measured *L*-subshell and total inner shell ionization cross-sections along with the other experimentally measured and calculated results are given in table 2 and also shown in figure 5. Our σ_{L_1} values are almost in agreement (lower by 20%) with that of the measured value due to Moheb *et al* [13]. Good agreement is seen between

Table 1. *L*-shell/subshell ionization cross-sections (in barn) of Au.

Energy (keV)		200	250	300	350
σ_{L_1}	P	0·0019	0·012	0·026	0·032
	E	0·0020*	0·024#	0·035#	0·065#
	T	0·0020++	0·015+	0·034++, 0·26$	0·41$
σ_{L_2}	P	0·00025	0·0024	0·0081	0·023
	E	0·00020*	0·0050#	0·013#	0·025#
	T	0·00034++	0·0028+	0·0089++, 0·12$	0·21$
σ_{L_3}	P	0·0029	0·017	0·064	0·11
	E	0·0020*	0·025#	0·060#	0·12#
	T	0·0035++	0·019+	0·069++, 0·71$	1·25$
σ_L	P	0·0050	0·031	0·098	0·165
	E	0·0042*	0·054#	0·108#	0·210#
	T	0·0059++	0·037+	0·11++, 1·09$	1·87$

P: Present measurement.
E: Measurement made earlier * – Ref. [11]; # – Ref. [9]
T: Theoretical calculations + –(RPWBA-BC) Ref. [16]; + + –(ECPSSR) Ref. [15]; $ – (PWBA) Ref. [14]

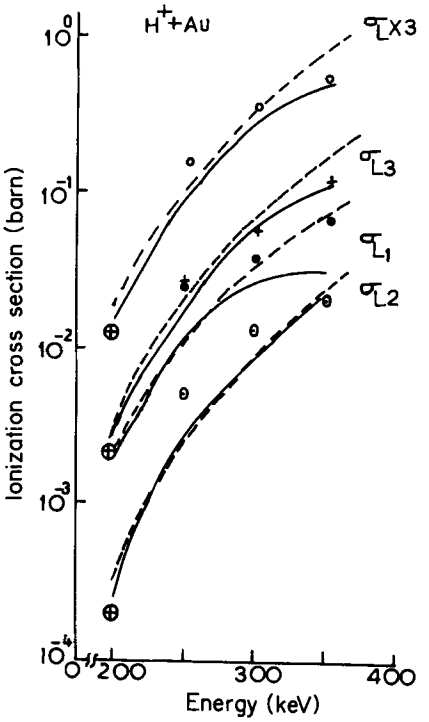

Figure 4. *L*-shell/subshell ionizations of Au due to proton impact. ——: Present results, ----: Ref. [15], (●) σ_{L_1}, (⊙) σ_{L_2}, (×) σ_{L_3}, (○) σ_L Ref. [9], (⊕) σ_L Ref. [11].

Table 2. *L*-shell/subshell ionization cross-sections (in barn) of Pb.

Energy (keV)		200	240	250	280	300	340	350
σ_{L_1}	P	0·0019		0·0071		0·018		0·033
	E		0·0069*		0·014*	0·021*	0·046*	
	T	0·00077++				0·017++ 0·16$		0·26$
σ_{L_2}	P	0·00045		0·0011		0·0035		0·0054
	E		0·00087*		0·0020*	0·0023*	0·0059*	
	T	0·00011++				0·0038++ 0·06$		0·12$
σ_{L_3}	P	0·0034		0·0075		0·019		0·042
	E		0·0040*		0·016*	0·028*	0·062*	
	T	0·0014++				0·035++ 0·43$		0·79$
σ_L	P	0·0057		0·016		0·040		0·080
	E		0·0118*		0·032*	0·051*	0·1139*	
	T	0·0023++				0·056++ 0·65$		1·17$

P: Present measurement.
E: Measurement made earlier * – Ref. [13];
T: Theoretical calculations + + – (ECPSSR) Ref. [15]; $ – (PWBA) Ref. [14]

the measurements and results reported by Cohen and Horigen [15] using the ECPSSR method for σ_{L_1} and σ_{L_2} cross-sections at 300 keV. The corresponding PWBA cross-sections [14] however, do not agree with our measured cross-sections. Present results for σ_{L_2} are in good agreement (though higher by 25%) with the cross-sections measured

Table 3. *L*-shell/subshell ionization cross-sections (in barn) of Bi.

Energy (KeV)		250	300	350
σ_{L_1}	P	0·0021	0·0029	0·0064
	T	$0·0054^{+}$	$0·013^{++}$	
σ_{L_2}	P	0·00098	0·0011	0·0034
	T	$0·00084^{+}$	$0·0028^{++}$	
σ_{L_3}	P	0·0045	0·0074	0·011
	T	$0·0066^{+}$	$0·027^{++}$	
σ_L	P	0·0076	0·011	0·021
	T	$0·013^{+}$	$0·043^{++}$	

P: Present measurement.
T: Theoretical calculations + – (RPWBA-BC) Ref. [16];
++ – (ECPSSR) Ref. [15]

Table 4. *L*-subshell ionization cross-section ratios for Au.

Energy (KeV)		200	250	300	350
$\sigma_{L_1}\sigma_{L_2}$	P	7·6	5·0	3·2	1·4
	E	10·0*	4·8#	2·7#	2·6#
	T	$5·9^{++}$	$5·4^{+}$	$3·8^{++}$ 2·2$^{\$}$	1·9$^{\$}$
$\sigma_{L_2}\sigma_{L_3}$	P	0·09	0·14	0·13	0·21
	E	0·10*	0·20#	0·22#	0·21#
	T	$0·097^{++}$	$0·15^{+}$	$0·13^{++}$ 0·17#	0·17$^{\$}$
$\sigma_{L_1}\sigma_{L_3}$	P	0·65	0·71	0·41	0·29
	E	1·0*	0·96#	0·58#	0·54#
	T	$0·57^{++}$	$0·79^{+}$	$0·49^{++}$ 0·37$^{\$}$	0·33$^{\$}$

P: Present measurement.
E: Measurement made earlier * – Ref. [11]; # – Ref. [9]
T: Theoretical calculations + – (RPWBA-BC) Ref. [16]; ++ – (ECPSSR) Ref. [15]; $ – (PWBA) Ref. [14]

by Moheb *et al* [13]. For the σ_{L_3}-subshell our values for the ionization cross-sections are close to the results of Moheb *et al* [13] but this agreement worsens as incident energy increases. Calculated σ_{L_3}cross-sections are two to three times lower at 200 keV but are larger by the same factor at 300 keV. Total inner shell ionization cross-section σ_L however, is found to be in good agreement with the earlier measured total cross-sections, though here also the agreement is poor towards higher incident energies.

The results of the subshell ionization cross-section ratios ($\sigma_{L_1}/\sigma_{L_2}$, $\sigma_{L_2}/\sigma_{L_3}$ and $\sigma_{L_1}/\sigma_{L_3}$) are given in table 5. It is found that our results are more or less similar to the values given by the ECPSSR theory [15]. Earlier measured values of $\sigma_{L_1}/\sigma_{L_2}$ ([13]) are approximately two times larger than the present results while our results for $\sigma_{L_2}/\sigma_{L_3}$ are two times larger than the corresponding values reported by Moheb *et al* [13]. In the case of $\sigma_{L_2}/\sigma_{L_3}$, the two sets of values are in reasonable agreement.

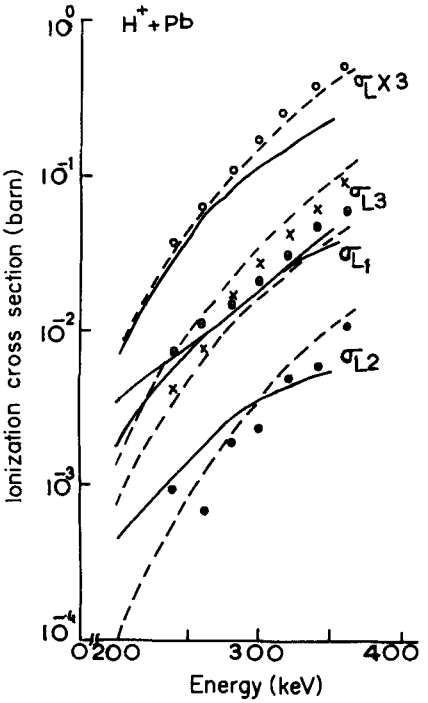

Figure 5. L-shell/subshell ionizations of Pb due to proton impact. ——: Present results, ----: Ref. [15] (○) σ_{L_1}, (●) σ_{L_2}, (×) σ_{L_3}, (○) σ_L Ref. [13].

Table 5. L-subshell ionization cross-section ratios for Pb.

Energy (KeV)		200	240	250	280	300	340	350
$\sigma_{L_1}/\sigma_{L_2}$	P	4·2		6·4		5·1		6·1
	E		7·9*		7·0*	9·1*	7·8*	
	T	7·0++				4·47++ 2·67$		2·17$
$\sigma_{L_2}/\sigma_{L_3}$	P	0·132		0·147		0·184		0·128
	E		0·217*		0·125*	0·082*	0·095*	
	T	0·078++				0·108++ 0·139$		0·152$
$\sigma_{L_1}/\sigma_{L_3}$	P	0·56		0·95		0·94		0·78
	E		1·72*		0·87*	0·75*	0·74*	
	T	0·55++				0·48++ 0·37$		0·33$

P: Present measurement.
E: Measurement made earlier * – Ref. [13]
T: Theoretical calculations + + – (ECPSSR) Ref. [15]; $ – (PWBA) Ref. [14]

Bismuth: Results of our measurements of the L-shell ionization cross-sections due to proton impact regarding Bi are given in table 3 and shown in figure 6. No earlier measurements are available. Therefore, only theoretically calculated cross-sections are available for comparison. From the table as well as the figure it is seen that our results for various subshells as well as the total ionization cross-sections are satisfactorily reproduced by the ECPSSR [15] at 300 keV. The cross-section ratio obtained using the RPWBA-BC [16] method at 250 keV are also seen to be in

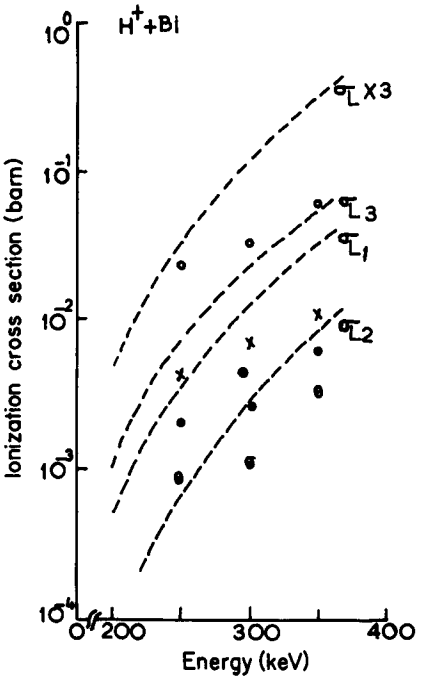

Figure 6. *L*-shell/subshell ionizations of Bi due to proton impact. (●), (⊙, ×, ○) Present results, ----: Ref. [15].

Table 6. *L*-subshell ionization cross-section ratios for Bi.

Energy (keV)		250	300	350
$\sigma_{L_1}/\sigma_{L_2}$	P	2·1	2·6	1·9
	T	$6{\cdot}43^{+}$	$4{\cdot}64^{++}$	
$\sigma_{L_2}/\sigma_{L_3}$	P	0·22	0·15	0·31
	T	$0{\cdot}13^{+}$	$0{\cdot}10^{++}$	
$\sigma_{L_1}/\sigma_{L_3}$	P	0·47	0·39	0·58
	T	$0{\cdot}81^{+}$	$0{\cdot}48^{++}$	

P: Present measurement.
T: Theoretical calculations + −(RPWBA-BC) Ref. [16]; + + −(ECPSSR) Ref. [15].

agreement with our measured values except for σ_{L_1} which is somewhat lower. Measured subshell ionization cross-sections (see table 6) are also in reasonable agreement with the calculated values except for $\sigma_{L_1}/\sigma_{L_3}$, in which case calculated values are comparatively large.

5. Conclusions

The agreement of the presently measured subshell and total inner shell ionization cross-sections for all the three systems with the previously measured and theoretically determined results are generally reasonable, considering the uncertainties in

fluorescence yields, Coster Krönig transition probabilities and relative widths. Therefore, functioning of our experimental set-up seems to be fairly reliable. In the case of Bi the reported result is the first experimental one regarding the low energy proton impact inner-shell ionization cross-section. Efforts in the direction of measuring the cross-sections for a large number of systems, in the same energy range are in progress.

Acknowledgments

The authors acknowledge the help received from Profs H Ehrhardt, K Bergmann and Dr K Jung of the University of Kaiserslautern, Germany. Discussions with Prof. A K Nigam, Drs L Chaturvedi and V J Menon are also gratefully acknowledged. These targets were provided by Prof. S K Parthasarathy (VECC, Calcutta) and the financial assistance by VW-Stifftung (Germany) and UGC (India).

References

[1] D Bhattacharya, S K Bhattacherjee and S K Mitra, *J. Phys.* **B13**, 967 (1980)
[2] J R Chen, J D Reber, David J Ellis and Thomas E Miller, *Phys. Rev.* **A13**, 941 (1976)
[3] J J Chmielewski, J L Flinner, F W Inmann, B Sollenberger and N V Udeh, *Phys. Rev.* **A29**, 29 (1981)
[4] S Fast, J L Flinner, A Glick, F W Inmann, L Oolman, C Pearso and D Wickelgren, *Phys. Rev.* **A26**, 2417 (1982)
[5] E Rosato, P Cuzzocrea, N De Cesare, E Perillo and G Spadaccini, *IEEE. Trans. Nucl Sci.* **NS30**, 967 (1983)
[6] A R Zander, *Nucl. Instrum. Methods* **280**, 483 (1985)
[7] P S Singh, H Mohan, D Singh, H R Verma and C S Khurana, *Indian J. Phys.* **A62**, 674 (1988)
[8] F Abrath and Tom J Gray, *Phys. Rev.* **A10**, 1157 (1974)
[9] S Datz, J L Duggan, L C Feldman, E Laegsgaard and J U Andersen, *Phys. Rev.* **A9**, 192 (1974)
[10] W Jitschin, A Kaschuba, R Hippler and H O Lutz, *J. Phys.* **B15**, 763 (1982)
[11] K Kiss, T Papo, J Palinkas, L Sarkadi and B Schilenk, *Acta Phys. Hung.* **58(1–2)**, 69 (1985)
[12] T K Li D L Clatk and G W Greenless, *Phys. Lett* **37**, 1209 (1976)
[13] H Moheb, R Bigaouette and F W Inmann, *Phys. Rev.* **A32**, 3739 (1985)
[14] K N Pandey, U S Tiwari and D N Tripathi, *Indian J. Phys.* **B63**, 133 (1990)
[15] D D Cohen and M Harrigan, *At. Data Nucl. Data Tables* **33**, 255 (1985)
[16] M H Chen and B Crasemann, *At. Data Nucl. Data Tables* **33**, 217 (1985)
[17] K N Pandey, R Shanker D N Tripathi and D K Rai, *Indian J. Technol.* **25**, 393 (1987)
[18] R S Sokhi and D Crumpton, *J. Phys.* **B19**, 4193 (1986)
[19] E Storm and H I Israel, *Nucl. Data Tables* **A47**, 565 (1970)
[20] M O Krause, *J. Phys. Chem. Ref. Data* **8**, 307 (1979)
[21] J H Scofield, *At. Data Nucl. Data* **14**, 121 (1974)
[22] B Buras and L Jelward, *Progress in crystal growth and characterization* [Recent advances in X-ray characterization of materials-II, edited by P Krishna (Pergamon Press, Oxford-New York, 1988) Vol 18, p 108
[23] R S Sokhi and D Crumpton, *Nucl. Instrum. Methods* **181**, 5 (1981)
[24] W Jitschin, R Hippler, K Fink, R Schuch and H O Lutz, *J. Phys.* **B16**, 4405 (1983)